

UNIVERSITY OF CALIFORNIA  
SANTA BARBARA

**The Electromagnetically Sustained Rhodes Piano**

by

Gregory Shear

A thesis submitted in partial satisfaction of the  
requirements for the degree of  
Master of Science

in

Media Arts & Technology

Committee in charge:  
Professor Curtis Roads, Chair  
Doctor Matthew Wright  
Professor Clarence Barlow  
Professor Ben Mazin

December 2011

The Thesis of Gregory Shear is approved:

---

Doctor Matthew Wright

---

Professor Clarence Barlow

---

Professor Ben Mazin

---

Professor Curtis Roads, Chair

---

Date

# The Electromagnetically Sustained Rhodes Piano

Copyright 2011

by

Gregory Shear

## **Abstract**

The Electromagnetically Sustained Rhodes Piano

by

Gregory Shear

The Electromagnetically Sustained Rhodes Piano is an augmentation of the original instrument with additional control over the amplitude envelope of individual notes. This includes slow attacks and infinite sustain while preserving the familiar spectral qualities of this classic electromechanical piano. These additional parameters are controlled with aftertouch on the existing keyboard, extending standard piano technique. We explain the physics behind the design of the original instrument and several methods that were investigated for driving oscillations in the mechanical tone generator, for controlling the amplitude of these oscillations, and for removing the strong driving signal that is picked up by the sensor from the audio output.

# Contents

<b>List of Figures</b>	<b>vii</b>
<b>List of Tables</b>	<b>viii</b>
<b>1 Introduction</b>	<b>1</b>
<b>2 Details of the Rhodes Piano</b>	<b>3</b>
2.1 The Tine and Tonebar . . . . .	4
2.1.1 Mechanics . . . . .	4
2.1.2 Spectral Character . . . . .	5
2.2 The Pickup . . . . .	6
2.2.1 Harmonic Distortion . . . . .	6
2.2.2 Voicing . . . . .	8
2.2.3 Electrical Circuit . . . . .	9
2.3 Summery . . . . .	10
<b>3 Prior Art</b>	<b>11</b>
3.1 The EBow . . . . .	11
3.2 The Electromagnetically-Prepared Piano . . . . .	12
3.3 Magnetic Resonator Piano . . . . .	13
3.4 Computerized Experiments with a Tuning Fork . . . . .	13
<b>4 Implementation</b>	<b>15</b>
4.1 Mounting the Electromagnet . . . . .	16
4.1.1 Model of Tonebar with Additional Point Mass . . . . .	17
4.1.2 Q Value and Frequency Variation . . . . .	18
4.1.3 Custom Tonebar Details . . . . .	19
4.2 Excitation . . . . .	19
4.2.1 Excitation Signal Source . . . . .	19
4.2.2 Phase Relationship Theory . . . . .	23
4.2.3 Excitation Circuit . . . . .	24
4.3 Aftertouch Control . . . . .	25
4.3.1 Force Sensitive Resistor . . . . .	25

4.3.2	FET Variable Attenuator . . . . .	25
4.3.3	Phototransistor FET Control . . . . .	26
4.4	Audio Output . . . . .	27
<b>5</b>	<b>Results and Evaluation</b>	<b>28</b>
5.1	Q Comparison and Frequency Variation . . . . .	28
5.2	Phase Theory Verification . . . . .	29
5.3	Timbre Comparison . . . . .	29
5.4	Excitation Signal Interference . . . . .	30
5.5	Example Amplitude Envelopes . . . . .	31
<b>6</b>	<b>Future Work</b>	<b>32</b>
6.1	Effective Frequency Range . . . . .	32
6.2	Adaptive Gain . . . . .	33
6.3	Percussive Attack and Active Damping . . . . .	33
6.4	Kit Production . . . . .	34
	<b>Bibliography</b>	<b>35</b>
	<b>A Tonebar Model</b>	<b>37</b>
	<b>B Mechanical-electrical signal path</b>	<b>40</b>

# List of Figures

2.1	Tone generator assembly. . . . .	3
2.2	Spectrogram of acoustic signal generated by vibrating tine. . . . .	6
2.3	Harmonic distortion of pickup signal compared with vibrating tine acoustic signal. . . . .	7
2.4	Example voltage signals generated by the pickup at various separations between tine and pickup axes. Fundamental at 196 Hz. . . . .	8
2.5	Harmonic distortion at various separations between tine and pickup axes. Fundamental at 196 Hz. . . . .	9
2.6	Example octave of series/parallel configuration of pickups. . . . .	10
4.1	Electromagnet coil on steel bolt. . . . .	16
4.2	Simple model of tonebar with attached actuator. . . . .	17
4.3	Custom tonebar with attached electromagnet and piezo sensor. . . . .	19
4.4	Electromagnet coils mounted above and below tonebars. . . . .	20
4.5	Excitation signal path block diagram. . . . .	24
4.6	Cascaded FET variable attenuators. . . . .	25
4.7	Partial diagram of alternating pickup array circuit. . . . .	27
5.1	Normalized spectra comparing passively decaying and actively sustained steady state oscillations. . . . .	30
5.2	Example amplitude envelopes. . . . .	31
A.1	Simple model of tonebar with attached actuator. . . . .	37
A.2	Separate cantilever beam and point mass models. . . . .	38
A.3	Effective masses at length $L_t$ of cantilever beam and actuator mass. . . . .	38
A.4	Aggregate effective mass on massless beam of length $L_t$ . . . . .	38
B.1	Complete excitation circuit diagram for one note. . . . .	42

# List of Tables

2.1	Example Q values for various notes in a 1974 Mark 1, 88-key Rhodes Piano. . . . .	5
4.1	Variable key and example values for Equation 4.1. . . . .	18
5.1	Q values for midrange notes, modified tine/tonebar systems in bold.	28

## Acknowledgments

# Chapter 1

## Introduction

Harold Rhodes first conceived of what would later be known as the Rhodes Piano in 1942 while serving in the United States Army Air Corps during World War II. Originally an acoustic instrument and assembled from surplus B-17 parts, the piano was designed for wounded soldiers to play from their hospital beds. After the war Harold Rhodes founded The Rhodes Piano Corporation and introduced an improved model of his piano at the first National Association of Music Merchants (NAMM) show in 1946. Thirteen years later Fender manufactured and sold the first Rhodes Piano in 1959 [1].

The Rhodes Piano sound has been familiar throughout mainstream music history and continues to be a staple of contemporary pop and electronica. Electronic artists in particular desire modern control affordances common to analog or computer based synthesizers, but extended control over the amplitude envelope of a Rhodes Piano was previously only achievable in the recording studio with non-

linear editing techniques. The Rhodes Piano is an electromechanical instrument that, like an electric guitar, requires amplification. Compression and variable gain stages preceding the amplifier offer limited real-time control over the amplitude envelope, but the audio signal originates from a passive vibrating mechanism inside the piano that experiences exponential decay after the initial percussive excitation. Swelling effects and infinite sustain remain out of reach for the Rhodes Piano in a live performance setting.

We present a novel system that offers greater control over the amplitude of this vibrating mechanism, including infinite sustain, and controlled by aftertouch on the original keyboard interface. Active electronics and custom hardware are retrofitted into the instrument extending its affordances while preserving the original functionality and characteristic timbre. Cost and ease of installation are also considered in hopes of producing a kit for users with minimal electronics experience to modify their own pianos. Rhodes enthusiasts may be wary of permanent alterations to their vintage instruments - these modifications are non-destructive and may be undone.

This research was first presented at the New Interfaces for Musical Expression conference in Oslo, Norway, 2011 [2].

## Chapter 2

### Details of the Rhodes Piano

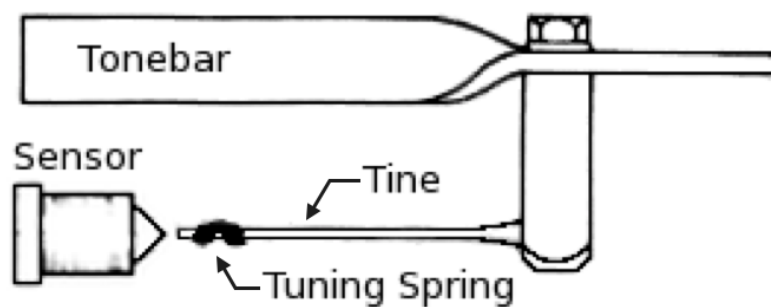


Figure 2.1: Tone generator assembly.

The Rhodes Piano [3] is an electromechanical instrument that generates an audio signal from a vibrating thin steel rod fixed at one end. This cantilever beam is called the *tine* and is shown in Figure 2.1. In each piano there is one tine per note with fundamental vibrating frequencies ranging from 41 Hz to 2.6 kHz on the 73-key model, and 27 Hz to 4.2 kHz on the 88-key model. Each tine is sensed by a dedicated passive magnetic pickup: Vibration in the tine disturbs the magnetic field through a coil of wire and generates an electrical signal (details of

this interaction can be found in Appendix B). The average (assuming all passive electrical components) of the signals from each pickup is present at the output jack of the instrument for amplification. Similar to an acoustic piano, the tine is struck from below by a hammer and damped by a felt pad. The particular instrument used in this project is an 88-key, Mark I stage piano from 1974.

## 2.1 The Tine and Tonebar

### 2.1.1 Mechanics

Each tine is paired with another cantilever beam, the *tonebar* - despite dissimilar physical dimensions their natural vibrating frequencies are matched and together they behave as an asymmetrical tuning fork [3]. The tine and tonebar are gross tuned by length while fine tuning for the pair is achieved with the *tuning spring* which adds mass at an adjustable position near the free end of the tine as shown in Figure 2.1. The tines range in length from 18 mm to 157 mm in the 88-key piano and are cylindrical with a diameter of 1.5 mm (except for slight widening at the base for strength).

The fundamental vibrating frequency of a cantilever beam can be calculated by its physical dimensions and material properties [4]:

$$f = 1.426 \frac{\pi K}{8L^2} \sqrt{\frac{E}{\rho}} \quad (2.1)$$

$$\text{where } K = \frac{h}{\sqrt{12}} \quad \text{for a rectangular cross section of height } h \quad (2.2)$$

Table 2.1: Example Q values for various notes in a 1974 Mark 1, 88-key Rhodes Piano.

Note	$f_0$ (Hz)	Q
E <sup>b</sup> 2	77.8	949
E <sup>b</sup> 3	155.6	731
E <sup>b</sup> 4	311.1	1520
E <sup>b</sup> 5	622.3	2175
E <sup>b</sup> 6	1244.5	1761

$$\text{or } K = \frac{r}{2} \quad \text{for a circular cross section of radius } r \quad (2.3)$$

The tuning fork behaves as a resonant filter and closely matched vibrating frequencies of each leg result in a higher Q value and slower dissipation of energy in the system:

$$Q = \frac{2\pi f_0 \tau}{2} \quad (2.4)$$

Where  $\tau$  is the time it takes for the signal to reach 37% of its original amplitude while vibrating at fundamental frequency  $f_0$  [5]. See Table 2.1 for example Q values of notes in the original piano. This long sustain was a selling point of the instrument and later models showed further improvements, particularly in the high frequency range.

### 2.1.2 Spectral Character

A piano string, which is fixed at both ends, vibrates with overtones at near integer multiples of the fundamental. In contrast, the tine is a cantilever beam and vibrates with decidedly inharmonic overtones at non-integer multiples of the fundamental [4]. Energy at these higher frequencies dissipates quickly, but although the inharmonic overtones are short lived, they give the Rhodes Piano a somewhat

bell-like timbre during the attack of each note. Beyond the initial attack, the tine settles in to simple harmonic motion with most of its vibrational energy at the fundamental frequency as shown in Figure 2.2.

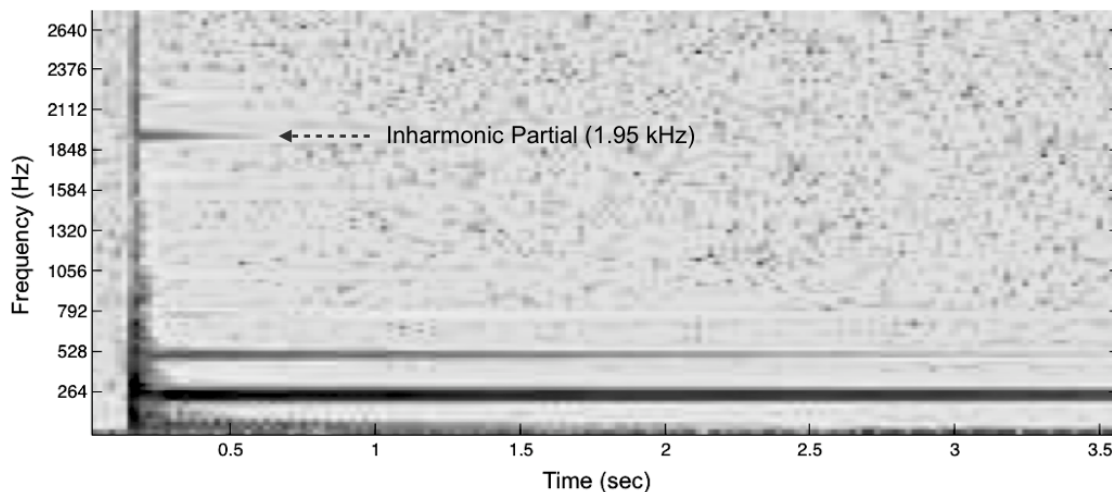


Figure 2.2: Spectrogram of acoustic signal generated by vibrating tine.

## 2.2 The Pickup

### 2.2.1 Harmonic Distortion

The pickup is a coil with  $N$  turns of wire wrapped around a permanent magnetic core. As the ferrous tine swings through the magnetic field surrounding the pickup, it disturbs the magnetic flux  $\Phi$  through the coil, generating an electromotive force  $\mathcal{E}$  in the coil.

$$V = \mathcal{E} = -N \frac{d}{dt} \Phi \quad (\text{Faraday's law}) \quad (2.5)$$

Assuming infinite resistance between the coil terminals with no current flowing, the voltage over the coil is equal to the electromotive force.

The magnetic field produced by the core is non-uniform and scales the value  $\frac{d}{dt}\Phi$  depending on the location of the tine within the field. This has the effect of modulating the voltage signal and introducing strong harmonic distortion which is clearly visible when comparing the spectra of the acoustic signal with the pickup signal during the decaying steady state tine oscillations. Figure 2.3 shows static spectra of the pickup signal compared to the acoustic signal of the vibrating tine where the fundamental peak in each series is set to 0 dB.

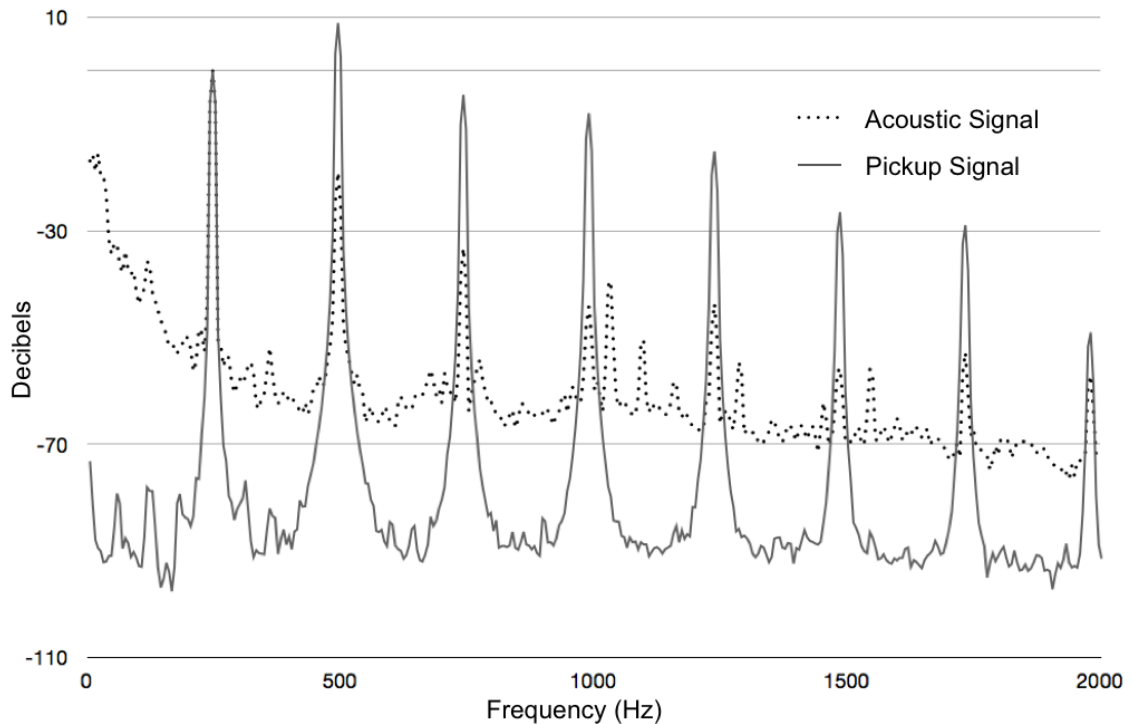


Figure 2.3: Harmonic distortion of pickup signal compared with vibrating tine acoustic signal.

## 2.2.2 Voicing

The harmonic distortion mentioned above is dependent on the vertical alignment of the tine and pickup: As the equilibrium point of the free end of the tine approaches the pickup axis, the fundamental and all odd partials are attenuated, leaving the second partial as the dominant frequency in the series. This vertical adjustment of the tine (in the direction of oscillation) is known as *voicing* and the effect is consistent with the findings in [6] where a modeled guitar string oscillates perpendicularly to the axis of its pickup (motion similar to that of our vibrating tine with respect to the pickup). The waveforms and frequency spectra produced by different tine alignments shown in Figure 2.4 and Figure 2.5 illustrate the effect of voicing adjustment.

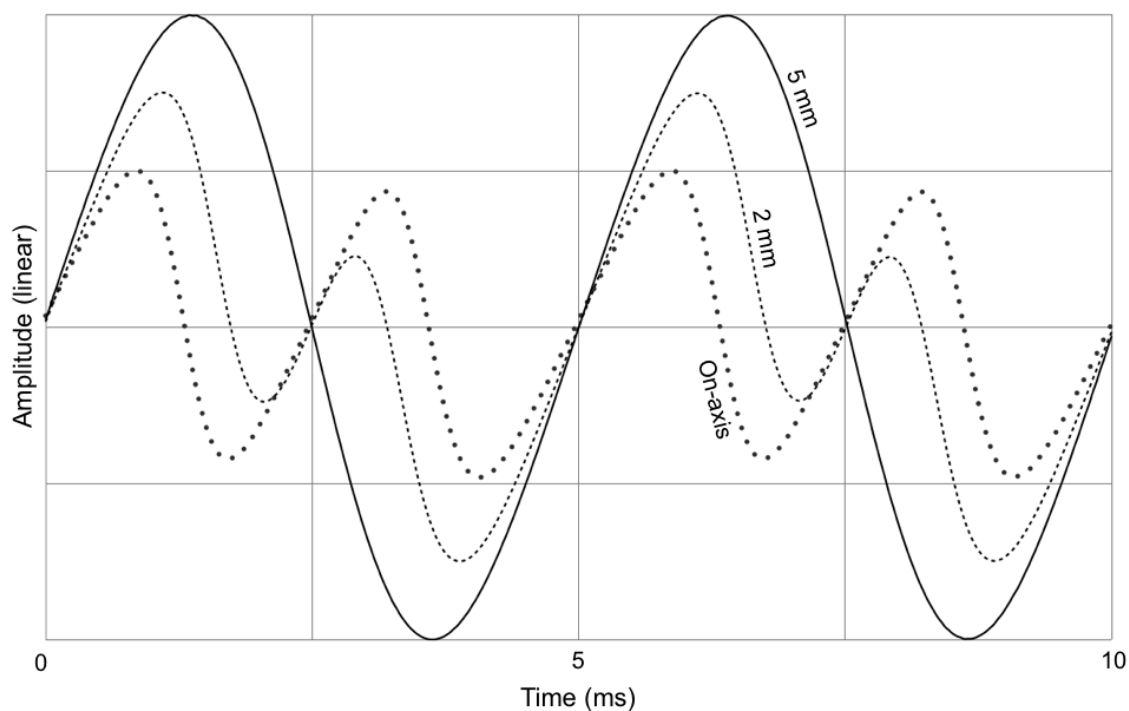


Figure 2.4: Example voltage signals generated by the pickup at various separations between tine and pickup axes. Fundamental at 196 Hz.

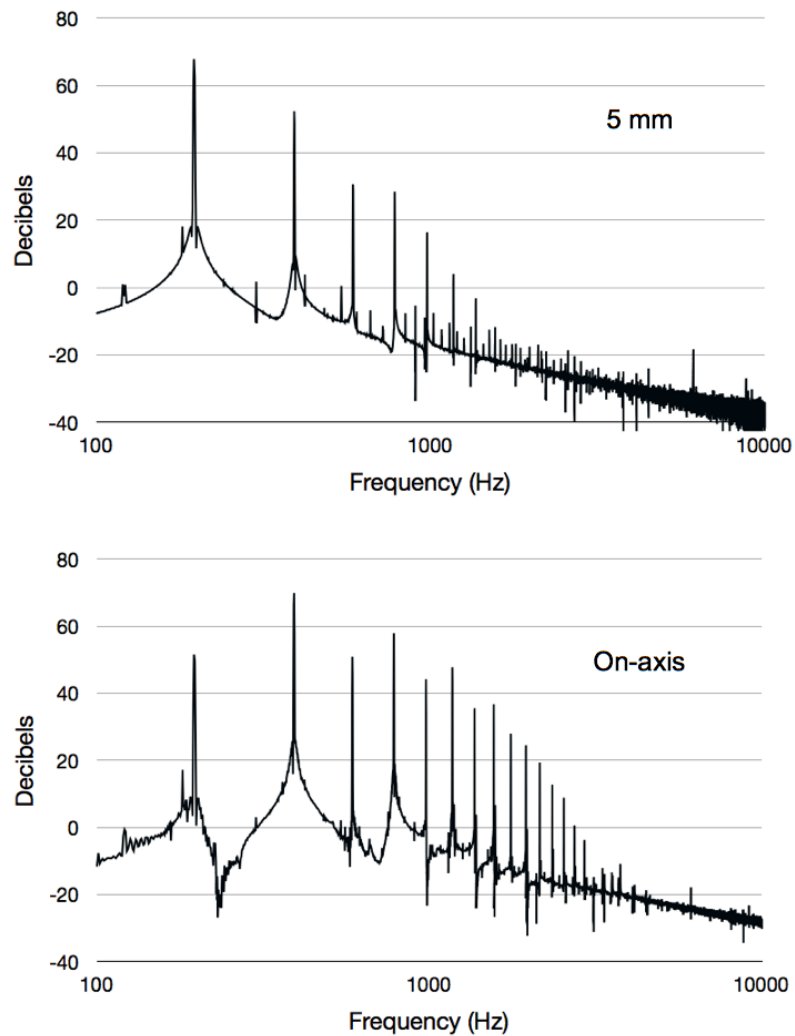


Figure 2.5: Harmonic distortion at various separations between tine and pickup axes. Fundamental at 196 Hz.

### 2.2.3 Electrical Circuit

Over the range of the keyboard the array of pickups is divided into parallel groups of three, and these groups are connected in series. Figure 2.6 shows a partial circuit diagram. The alternating polarity of each group reduces electromagnetic interference in the output audio signal [3].

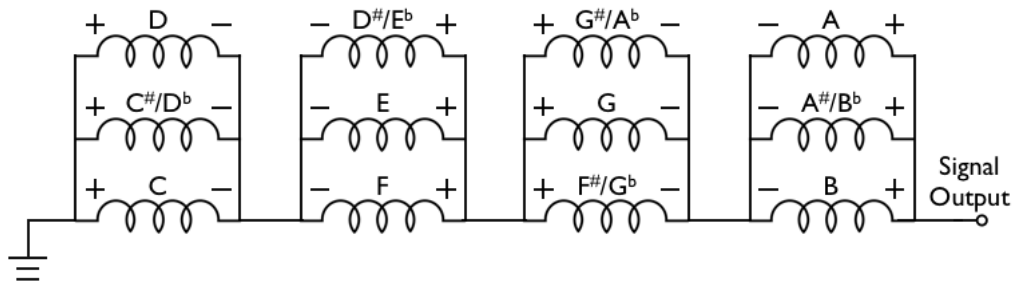


Figure 2.6: Example octave of series/parallel configuration of pickups.

## 2.3 Summery

This understanding of the mechanics and electronics theory behind the Rhodes Piano allows us to begin planning our modifications in hopes of minimizing unwanted side effects.

# Chapter 3

## Prior Art

There are relatively few instruments and devices that take on a similar challenge to ours - actively sustaining vibrations in a string or tuning fork for musical applications. The following examples all share a similar component: The electromagnet. Beside this they offer a range of ideas and techniques for us to choose from or find necessary alternatives to.

### 3.1 The EBow

The EBow is a handheld electronic device that sustains vibrations in ferromagnetic guitar strings through positive feedback [7]. The guitarist controls the device by moving it toward or away from the strings. The EBow uses one coil (the pickup) to generate a signal that drives a second coil (the electromagnet) which in turn exerts a time-varying magnetic force on the string supporting its oscillation. Permanent magnetic cores in each coil temporarily magnetize the ferromagnetic

string greatly increasing efficiency of the actuator and allowing for both attractive and repulsive forces between the actuator and string. Without this magnetization, the actuator would exert only an attractive force on the string, effectively rectifying the actuator signal.

This project began with simple experiments where we held an EBow near the tines of a Rhodes Piano. This successfully initiated and sustained oscillations proving the tines could be excited with an electromagnetic actuator compact enough to fit in the limited space inside the piano.

## **3.2 The Electromagnetically-Prepared Piano**

The Electromagnetically-Prepared Piano (EMPP) [8] is an acoustic grand piano with electromagnetic actuators placed above certain strings. Each actuator is driven with an arbitrary audio signal (the creators suggest pure sine waves, orchestral samples, noise, etc.) through a standard audio amplifier. This signal is transmitted to the strings via the magnetic force exerted by the electromagnet, and the strings in turn transmit the signal to the piano soundboard. Control is achieved through software such as Cycling 74s Max/MSP [9] leaving the original key/hammer action unaltered.

This differs from our system in that our excitation signal is generated by the vibrating mechanism itself thus completing a feedback loop, and we control the system through sensors retrofitted to the existing keyboard interface.

### **3.3 Magnetic Resonator Piano**

Our project is modeled after Andrew McPherson's Magnetic Resonator Piano (MRP) - a grand piano with extended timbral and amplitude envelope control through continuous position sensing of individual keys [10]. Excitation signals for individual notes originate at a single piezo-electric sensor placed on the soundboard. This signal is distributed to a series of tuned bandpass filters that then drive electromagnetic actuators positioned above the strings, similar to the Electromagnetically-Prepared Piano. An adjustable delay compensates for the propagation time through the soundboard and the resulting phase difference between the velocity of the string and the force exerted by the electromagnet. Continuous sensing is achieved with a modified Moog Piano Bar [11] and a complex scheme of this control data maps key position to amplitude and spectral parameters for each note.

### **3.4 Computerized Experiments with a Tuning Fork**

Kraftmakher describes an apparatus for demonstrating free and forced oscillations in the classroom where an actuator coil initiates and sustains oscillations in a standard tuning fork [?]. He first drives the actuator coil with a synthesized sine wave at frequencies at and near to the natural vibrating frequency of the tuning fork. Stronger physical vibrations are produced as the synthesized sine frequency approaches the natural frequency of the tuning fork, and amplitude beating is observed as the synthesized signal deviates from the natural frequency.

Kraftmakher also creates a mechanical-electrical feedback loop driving the actuator coil with an amplified microphone signal from the vibrating tuning fork. With the exception of the sensing method, this system is most similar to our current design despite having such unrelated motivations.

# Chapter 4

## Implementation

Given the assortment of instruments and devices described in Chapter 3, the use of electromagnetic actuators is not only obvious, but remains the only feasible way of electronically initiating and sustaining oscillations in ferromagnetic strings or tuning forks. As described in Sections 2.1 and 2.2, the characteristic sound of the Rhodes Piano depends both on the inharmonic overtones of the vibrating tine and the strong harmonic distortion added by the magnetic pickup. These three indispensable components, the tine, the pickup, and the electromagnet, are at odds with each other: Compared to piano or guitar strings, the tines in a Rhodes Piano are very short, forcing close proximity between electromagnet and pickup. Interference is inevitable in this arrangement and must be compensated for.

Mounting the electromagnets is easy in an acoustic grand piano where the lid may be propped open or removed entirely, exposing the strings with ample space above for hardware. The tonebars in a Rhodes Piano, however, block access to the

tines from above, and the standard hammer action occupies the space below. The only place for additional components is between the tonebar and the tine - far away from a solid anchor point to mount a suspension arm and very close to sensitive moving parts. Furthermore, the electromagnets are too wide to fit next to each other without lengthwise staggering that would vary their ability to move the tine.

## 4.1 Mounting the Electromagnet

The electromagnet, seen in Figure 4.1, is a coil of approximately 450 turns of 30 AWG copper wire wound around a plastic sewing machine bobbin. A steel bolt serves as the core and the coil has a DC resistance of 8 ohms. Attaching



Figure 4.1: Electromagnet coil on steel bolt.

the electromagnet directly to a custom tonebar minimizes the mounting hardware necessary to suspend the electromagnet above the tine and maintains the critical separation between the electromagnet and tine during voicing adjustments. The

additional mass of the electromagnet lowers the fundamental vibrating frequency of the tonebar and must be compensated for by shortening the tonebar length.

#### 4.1.1 Model of Tonebar with Additional Point Mass

In order to calculate the length of the new tonebar with the additional electromagnet mass  $m_e$  we suggest a simple model of an ideal cantilever beam (with mass) of length  $L_t$  and a point mass attached at distance  $L_e$  from the base, shown in Figure 4.2 [12]. This model leads us to Equation 4.1 with  $L_t$  in terms of known dimensions and material properties. See Table 4.1 for a variable key and example values and Appendix A for the derivation.

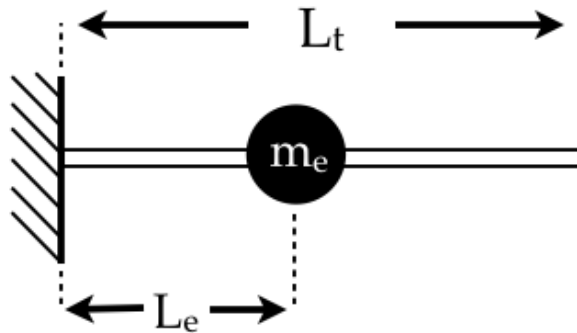


Figure 4.2: Simple model of tonebar with attached actuator.

$$L_t^4 = \frac{\frac{3EK}{(2\pi f_0)^2} - m_e L_e}{0.346wh\rho} \quad (4.1)$$

Table 4.1: Variable key and example values for Equation 4.1.

Tonebar Length	$L_t$	0.0821 m
Tonebar Width	$w$	0.0111 m
Tonebar Height	$h$	0.0034 m
Young's Modulus	$E$	$69 \times 10^9$ Pa
Density	$\rho$	2700 kg/m <sup>3</sup>
Electromagnet Mass	$m_e$	0.030 kg
Electromagnet Position	$L_e$	0.0268 m
Fundamental Frequency	$f_0$	293.7 Hz (D4)

### 4.1.2 Q Value and Theoretical Frequency Variation

The fundamental vibrating frequency varies between damped and undamped oscillations where the frequency ratio depends on the damping coefficient  $\zeta$ :

$$\frac{f_{damped}}{f_{undamped}} = \sqrt{1 - \zeta^2} \quad (4.2)$$

$$\text{where } \zeta = \frac{1}{2Q} \quad (4.3)$$

Human hearing has the highest frequency resolution in the 1 kHz to 3 kHz range where the just noticeable difference (JND) is about 0.5%<sup>1</sup> for a sine tone [13][14]. To stay within this 0.5% tolerance of human perception of frequency, the damping coefficient of the modified tine and tonebar system must be no greater than 0.10. By Equation 4.3, this corresponds to a minimum Q value of 5. Q values of original tine/tonebars are above 1000 in this range. Perceptible frequency shift will not likely be an issue with the modified system.

---

<sup>1</sup>Approximately 8.6346 cents.

### 4.1.3 Custom Tonebar Details

The new tonebar is machined out of a piece of 6061 aluminum and is pictured in Figure 4.3 with attached electromagnet. The coil may also be mounted on top with the core extending through the tonebar to carry the magnetic field down to the tine. Alternating coils above and below the tonebars allows the electromagnets to be placed directly next to each other as shown in Figure 4.4.

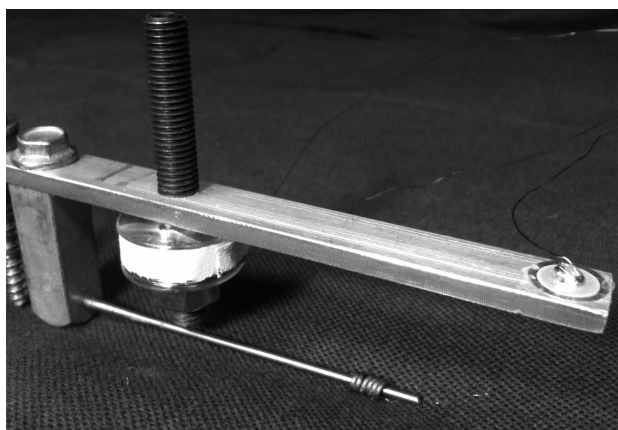


Figure 4.3: Custom tonebar with attached electromagnet and piezo sensor.

## 4.2 Excitation

### 4.2.1 Excitation Signal Source

While the similarity between all of the prior art examples discussed in Chapter 3 was the use of an electromagnet to drive oscillation in the vibrating mechanism, the way they are all different from each other is the source of the excitation signal. The EBow uses a magnetic pickup, the Electromagnetically-Prepared Piano ex-

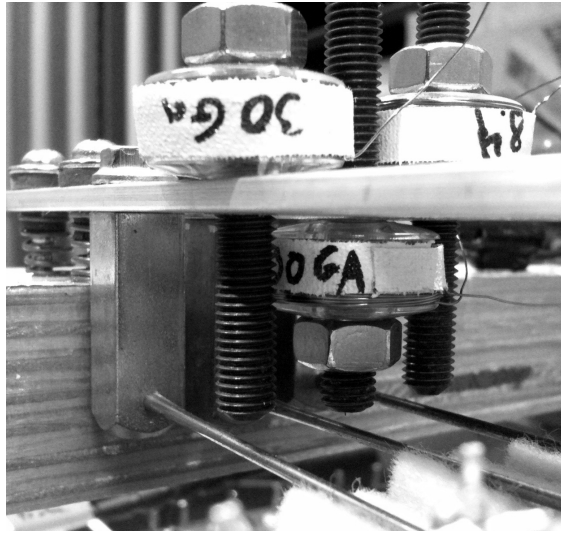


Figure 4.4: Electromagnet coils mounted above and below tonebars.

cites its strings with arbitrary prerecorded or synthesized waveforms, the Magnetic Resonator Piano senses vibrations with a piezo-electric sensor, and the classroom tuning fork apparatus uses a microphone. We investigated the first three of these possibilities and the advantages and disadvantages of each method are explained in detail below.

### **Synthesized Sine Wave**

Driving the actuator with a pure sine wave at the tine's fundamental frequency effectively initiates and sustains oscillations in the tine. In fact, this has been a necessary procedure for testing different parts of the system. As expected, the electromagnetic excitation signal is sensed by the pickup and dominates the audio signal but is easily subtracted with a relatively simple circuit that compensates for phase shift and amplitude scaling at the particular operating frequency. Still,

even a small difference between the synthesized frequency and the natural vibrating frequency of the tine produces perceptible amplitude beating while the tine settles into its steady state oscillations, consistent with the findings in [?]. Furthermore, we found no obvious way to inexpensively synthesize enough excitation signals in separate channels to make this scalable up from one note.

### **Pickup Signal**

Sensing vibrations in the tine to generate the excitation signal solves the problem of slightly detuned frequencies and the resulting amplitude beating. Driving the electromagnet with the audio signal also excites the tine from rest with amplified system noise. The high electrical gain needed in the circuit produces unruly electromagnetic feedback between the electromagnet and pickup - removing the excitation signal is necessary in this case not only for preserving the timbre of the instrument but also for controlling the feedback loop. Given the richness of this excitation signal, a simple circuit will not compensate for the frequency dependent phase shift introduced by the pickup as it did for a pure sine tone.

A second matched pickup placed near the fixed end of the tine also senses the electromagnetic field and, with the same frequency response, produces the same signal as the first pickup but without the tine component. The tine component may then be isolated by differential cancellation of the two pickup signals. Please note that the distortion described in Section 2.2.1 is an effect of the tine moving through the non-uniform magnetic field produced by the pickup and no such modulation is

imposed on the excitation signal emitted by the electromagnet and sensed by the pickup.

While this method works well for a single note [2], there are several drawbacks. Voicing adjustments change the amount of the fundamental frequency present in the excitation signal and therefore the amount of electrical gain necessary to drive oscillations in the tine. The requirement of a second matched pickup greatly increases cost and difficulty of retrofitting the system into the original piano. Finally, the subtraction signal produced by the second pickup has the appropriate amplitude when this pickup is the same distance from the electromagnet as the first pickup - adjacent electromagnets will not share this one-to-one relationship and the subtraction signal will not fully remove this additional interference.

### **Piezo Sensor Signal**

A piezo-electric sensor mounted to the end of the tonebar (shown in Figure 4.3) produces a nearly perfect sine wave as the tine and tonebar vibrate together at the same frequency. These sensors are small, light, easily mounted to the tonebar, unaffected by voicing adjustments and immune to the electromagnetic field. At about \$1 US each, they are by far the cheapest source for the excitation signal.

## 4.2.2 Phase Relationship Theory

The vibrating tine is a damped harmonic oscillator that experiences a restoring force  $-kx$  and a damping force  $-cv$ :

$$F_{net} = -kx - cv \quad (4.4)$$

To sustain oscillations at a constant amplitude, a magnetic force must be exerted on the tine equal and opposite to the damping force so that the net force is equal to that experienced by an ideal, undamped oscillator:

$$F_{net} = -kx - cv + cv = -kx \quad (4.5)$$

$$F_{mag} = cv \quad (4.6)$$

Equation 4.6 shows that the magnetic force must be proportional to and in phase with the *velocity* of the tine. The piezo sensor, however, behaves as an accelerometer and produces a voltage signal proportional to and in phase with the *acceleration* of the tine. Steady state oscillations of the tine are predominantly sinusoidal and the resulting phase relationship between velocity and acceleration is  $90^\circ$  - a difference that must be compensated for somewhere in the signal path from the source to the exerted force on the tine. The only phase shift introduced along this electrical-mechanical signal path is in the electronic circuit (detailed explanation found in Appendix B) where we can add an adjustable delay to make this compensation.

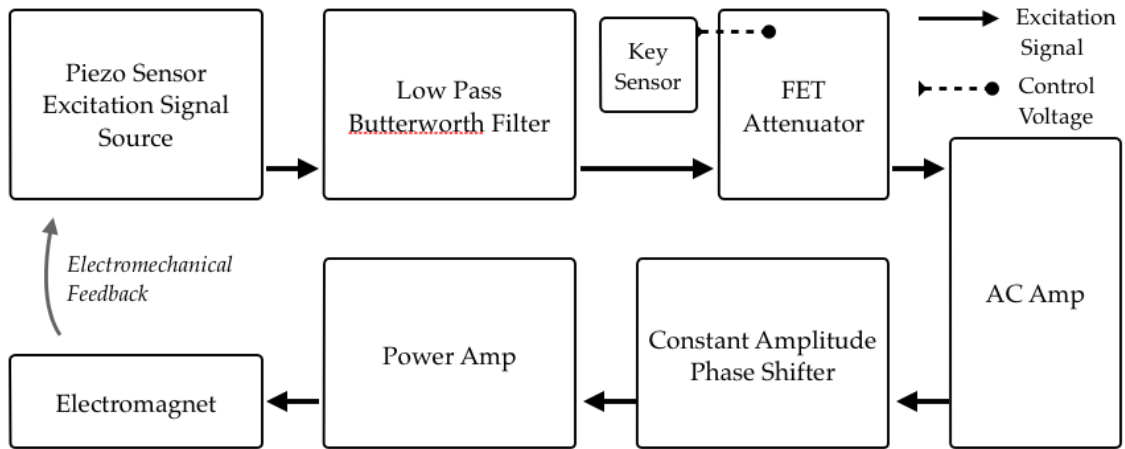


Figure 4.5: Excitation signal path block diagram.

### 4.2.3 Excitation Circuit

Figure 4.5 shows a block diagram of the excitation signal path, beginning at the piezo sensor. The lowpass filter cutoff frequency is set at XX Hz and stabilizes the feedback loop without attenuating the fundamental excitation frequency. The attenuator is controlled by a voltage from an optical key position sensor as described in Section 4.3.3. The AC amplifier provides gain and blocks a DC bias introduced by the attenuator. The constant amplitude phase shifter adjusts the overall delay of circuit and allows the phase relationship between piezo sensor voltage and the force exerted on the tine to be set to the desired  $90^\circ$  as described in Section 4.2.2.

A detailed circuit diagram can found in Appendix B.

## 4.3 Aftertouch Control

### 4.3.1 Force Sensitive Resistor

Force Sensitive Resistors (FSRs) beneath the keys in the existing Rhodes Piano keyboard is the simplest way to achieve aftertouch control for individual notes. At the bottom of the range of motion, the key comes in contact with and applies pressure to an FSR on the key bed where more pressure resulted in less resistance. Our first attempt put this variable resistance in the excitation signal path, introducing high frequency noise into the excitation signal that was not easily cancelled from the audio signal.

### 4.3.2 FET Variable Attenuator

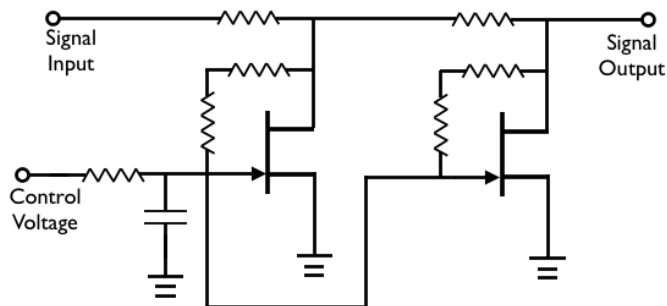


Figure 4.6: Cascaded FET variable attenuators.

A field effect transistor behaves like a voltage controlled variable resistor for small voltage signals [15]. Our second attempt at variable gain used the FSR to provide a control voltage for two cascaded FET variable resistors connected to ground (see Figure 4.6). These effectively turn the electromagnet off when no

pressure is applied to the FSR and a lowpass filter on the control voltage prevents clicks and crackling from abrupt amplitude changes.

This circuit works well but the FSR components are very expensive - at approximately \$6 US each they are one of the most expensive parts in the entire system. With one FSR necessary for every note on the keyboard, this is a prohibitive cost.

### 4.3.3 Phototransistor FET Control

The QRD1114 Reflective Object Sensor is a small component containing an LED and a phototransistor where the output voltage varies as light reflects off a nearby object and is received by the phototransistor [16]. This part and a dual op-amp for signal conditioning provide a sufficient control voltage for the previous FET variable attenuator circuit, but cost under \$2 US - much less expensive than the FSR.

The phototransistor provides continuous sensing of key position throughout its entire range of motion. At the bottom of this range, the key/hammer action flexes and the key moves closer to the phototransistor by a few more millimeters, depending on how much force is exerted on the they key. The Moog Piano Bar uses similar optical sensors and the Magnetic Resonator Piano relies on the same movement of the piano key to achieve aftertouch tremolo effects [10]. This movement results in a voltage change of up to 0.5 V which, with a DC offset and inverting gain, can be mapped to a control voltage of  $-6\text{ V}$  to  $0\text{ V}$  for the FET.

Aftertouch produces a small movement compared to the entire range of motion

of the key, all of which is sensed by our current system. Although we ignore the control signal outside of this small aftertouch range, Chapter 6 offers ideas for future modifications that will utilize the full control signal.

## 4.4 Audio Output

Similar to the original configuration, the pickups are wired in an alternating polarity pattern to reduce electromagnetic interference in the audio output signal. We reverse the polarity on every other pickup, instead of parallel groups of three, and buffer all of the signals before summing for improved signal to noise ratio. A partial circuit diagram is shown in Figure 4.7.

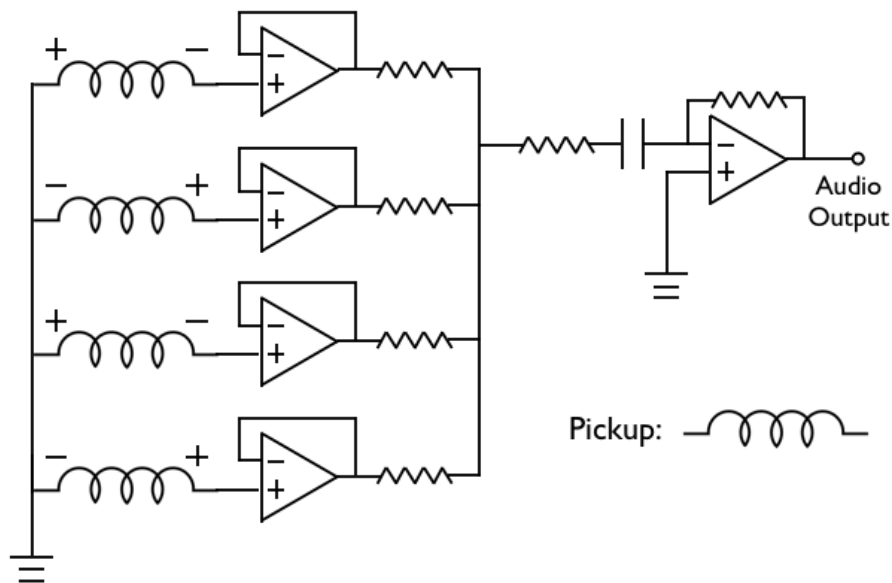


Figure 4.7: Partial diagram of alternating polarity pickup array circuit.

# Chapter 5

## Results and Evaluation

Here we present a few objective measurements that illustrate our successes and suggest a direction for future efforts.

### 5.1 Q Comparison and Frequency Variation

Table 5.1: Q values for midrange notes, modified tine/tonebar systems in bold.

Note	$f_0$ (Hz)	Q
B3	246.9	1101
<b>C4</b>	<b>261.6</b>	<b>1238</b>
<b>D<sup>b</sup>4</b>	<b>277.1</b>	<b>1040</b>
<b>D4</b>	<b>293.7</b>	<b>1156</b>
E <sup>b</sup> 4	311.1	1520

Table 5.1 contains Q values for original and modified tine/tonebar systems in the midrange of the piano - our modifications have had no appreciable effect on the inherent decay properties in this range.

Our lowest Q value of 1040 for D<sup>b</sup>4 would result in a frequency shift of less

than 0.000012% between inherently damped and actively sustained oscillations - a frequency difference completely imperceptible by humans.

## 5.2 Phase Theory Verification

As described in Section 4.2.2, we desire a magnetic force proportional to the velocity of the tine and  $90^\circ$  out of phase with the piezo sensor (accelerometer) signal. The only delay in the mechanical-electrical signal path (detailed in Appendix B) is introduced in the circuit and can be measured. An oscilloscope easily compares the input voltage and output current (measured by the voltage over a  $1\Omega$  resistor between the electromagnet and ground - see Appendix B). Indeed, adjusting the phase shifter to achieve a  $90^\circ$  phase difference between input and output signals results in the highest amplitude oscillations during active sustain.

## 5.3 Timbre Comparison

The frequency spectrum of the actively sustained tine signal is similar to that of the passively vibrating tine signal (see Figure 5.1). The fundamental frequency is less prominent compared to the upper harmonics during the actively sustained note. This may be a result of interference of the excitation signal described below in Section 5.4.

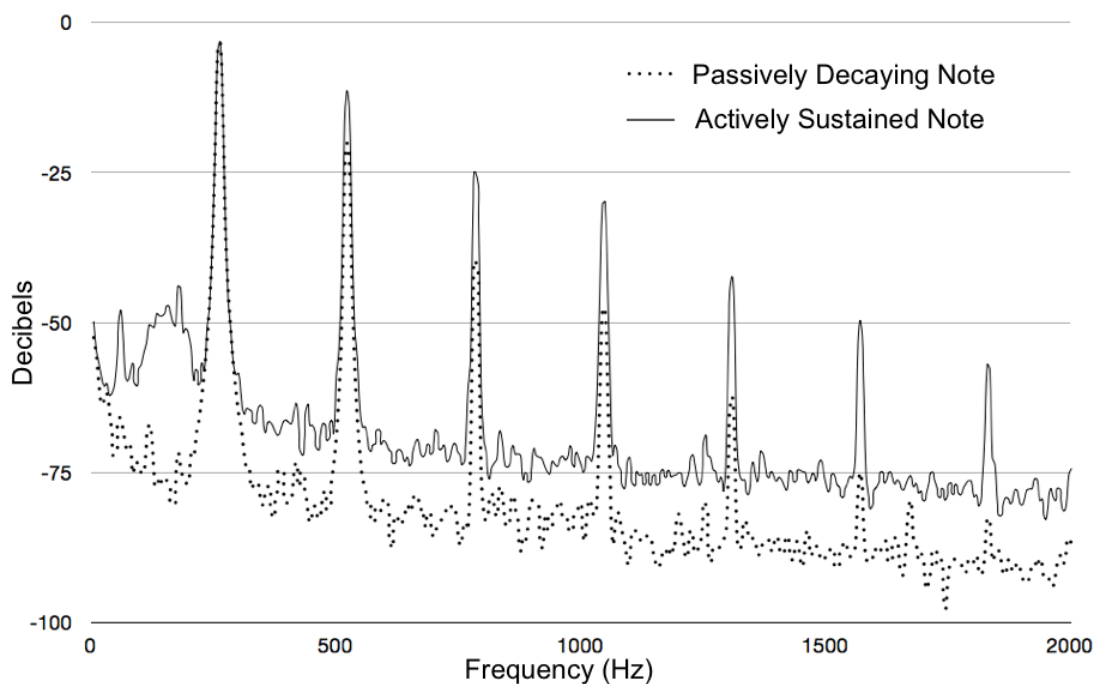


Figure 5.1: Normalized spectra comparing passively decaying and actively sustained steady state oscillations.

## 5.4 Excitation Signal Interference

We tested the cancellation method by holding the tine motionless and then driving the electromagnet with a synthesized sine wave. With the same polarity, each pickup in the array would add the excitation signal to the audio output. Our alternating pickup array produces a signal approximately equal to that of only the pickup nearest to the electromagnet. Destructive interference is removing a significant portion of the unwanted excitation signal from the audio output.

This residual excitation signal in the audio output is approximately  $180^\circ$  out of phase with the signal produced by the vibrating tine. This explains the relative attenuation of the fundamental peak in the active sustain frequency spectrum seen in Figure 5.1.

## 5.5 Example Amplitude Envelopes

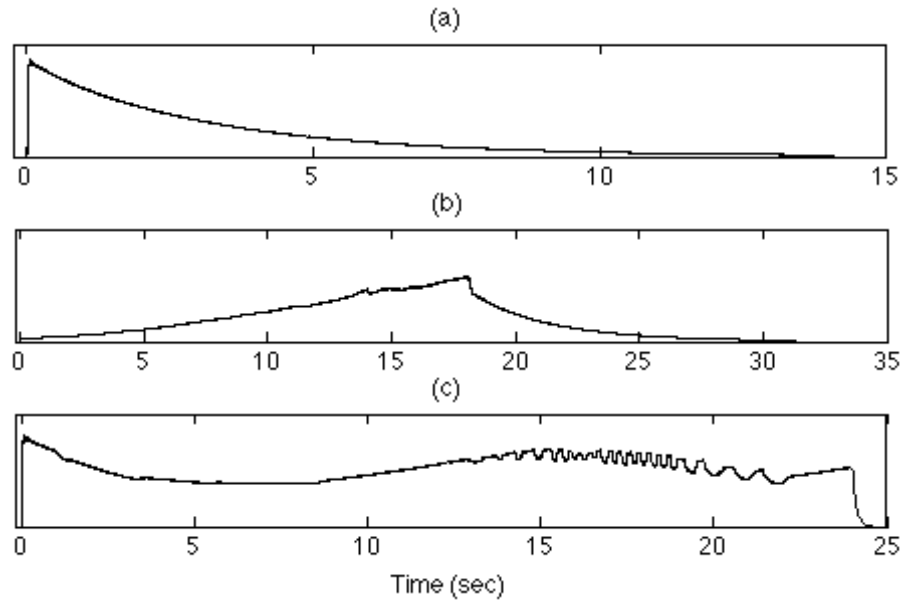


Figure 5.2: Example amplitude envelopes.

Figure 5.2 shows example amplitude envelopes produced by the instrument: (a) is a standard hammer attack with natural, unsustained decay; (b) also decays naturally, but reaches peak amplitude only by electromagnetic actuation; (c) is a standard hammer attack followed by tremolo and shortened decay by the felt damper.

# Chapter 6

## Future Work

### 6.1 Effective Frequency Range

The current system works well in the middle octave of the piano, but the extreme high and low end will present new challenges. As described in Section 2.1, the highest frequency tines are as short as 18 mm and the attached tonebars are correspondingly short and we do not yet know if our method of mounting the electromagnet directly to the tonebar will be possible in this range. We are also unsure if the excitation signal will cancel as nicely given the tight proximity between electromagnet and pickup at this end of the piano.

At the low end, the long tines reach a much greater maximum deflection from equilibrium when vibrating at full amplitude, so much so that the original tonebars were reshaped to provide clearance. Furthermore, on the 88 key piano, the lowest seven tines have no tonebars at all. We don't fully understand the vibration me-

chanics involved at this end of the piano - more research will be necessary before we determine what modifications are feasible on these notes.

## **6.2 Adaptive Gain**

One disadvantage to electrical-mechanical feedback is the variation in amplitude of the excitation signal. At high amplitude tine oscillations, the piezo sensor produces a correspondingly high amplitude voltage signal and relatively low gain is needed to amplify this signal and sustain oscillations. When exciting the tine from rest, on the other hand, very high gain is needed to amplify system noise to initiate oscillations. This high level of gain causes the excitation signal generated at full amplitude tine oscillations to clip, introducing high frequency distortion that can be heard in the audio output. If the performer is aware of this possibility, she may ease off on aftertouch pressure as amplitude increases, but adaptive gain limiting will prevent this undesirable affect all together.

## **6.3 Percussive Attack and Active Damping**

We have done a some basic experiments where the electromagnet polarity is reversed and as expected oscillations decayed much faster than the passively vibrating (and inherently damped) tine. The electromagnet will switch modes when the key returns to its upper position - the continuous phototransistor based sensing system described in Section 4.3.3 already provides the control signal necessary for

this implementation. We also speculate higher gain and minimal delay in the signal path will improve this damping method and eventually replace the felt dampers.

With a more powerful amplifier, we hope to excite the tine with a square pulse for a percussive attack and achieve the traditional sound of the Rhodes Piano without the mechanical key/hammer action. The high frequencies associated with a square pulse may not cancel from the audio signal with the current system - some amount of bandlimiting may be necessary, though it is possible that an audible click during the attack of a percussive note would be desirable. A control signal corresponding to key velocity could be obtained by differentiating the key position voltage already produced by the phototransistor. The velocity would have to reach a certain threshold to trigger the pulse, and then variation in the velocity above this threshold would control the amplitude of the pulse.

Percussive attack and active damping with the electromagnet will also allow the instrument to be played with an external controller. We envision a future Rhodes sound module with no keyboard that would respond to MIDI or OSC data.

## 6.4 Kit Production

In the immediate future we hope to begin printing circuit boards and experimenting with different Rhodes Pianos from various production years to see how well the current system integrates to the range of models. We will also be refining the circuit and removing unnecessary components to reduce cost and simplify the build process.

# Bibliography

- [1] Rhodes Music Corporation. History. <http://www.rhodespiano.com/history.htm>, 2011.
- [2] G. Shear and M. Wright. The electromagnetically sustained Rhodes piano. In *NIME Proceedings*, Oslo, Norway, 2011.
- [3] Rhodes Keyboard Instruments USA. *Rhodes Service Manual*, 1979.
- [4] T. D. Rossing and N. H. Fletcher. *Principles of vibration and sound*. Springer, 2nd edition, 2004.
- [5] W. M. Siebert. *Circuits, Signals, and Systems*. MIT Press, 1986.
- [6] N.G. Horton and T.R. Moore. Modeling the magnetic pickup of an electric guitar. *American Journal of Physics*, 77:144, 2009.
- [7] G Heet. String instrument vibration and sustainer, 1978. U.S. Pat. 4,075,921.
- [8] E. Berdahl, S. Backer, and J. Smith. If I had a hammer: Design and theory of an electromagnetically-prepared piano. In *ICMC Proceedings*, Barcelona, Spain, 2005.

- [9] D. Zicarelli. An extensible real-time signal processing environment for Max. In *ICMC Proceedings*, Ann Arbor, Michigan, USA, 1998.
- [10] A. McPherson and Y. Kim. Augmenting the acoustic piano with electromagnetic string actuation and continuous key position sensing. In *NIME Proceedings*, Sydney, Australia, 2010.
- [11] PianoBar. Products of interest. *Computer Music Journal*, 29(1):104–113, 2005.
- [12] T. Irvine. Bending frequencies of beams, rods, and pipes. <http://www.vibrationdata.com/tutorials2/beam.pdf>, 2011. Revision P.
- [13] J. Benesty, M. M. Sondhi, and Y. Huang, editors. *Springer Handbook of Speech Processing*. Springer, 2007.
- [14] G. Loy. *Musimathics*, volume 1. MIT Press, 2006.
- [15] P. Horowitz and W. Hill. *The Art of Electronics*. Cambridge University Press, 2nd edition, 1989.
- [16] Qrd1114 reflective object sensor datasheet. <http://www.fairchildsemi.com/ds/QR/QRD1114.pdf>.

# Appendix A

## Tonebar Model

Here we explain the simple model of an ideal cantilever beam (with mass) of length  $L_t$  and a point mass  $m_e$  attached at distance  $L_e$  from the base, shown in Figure A.1. The point mass can be considered separately as a mass at the end of

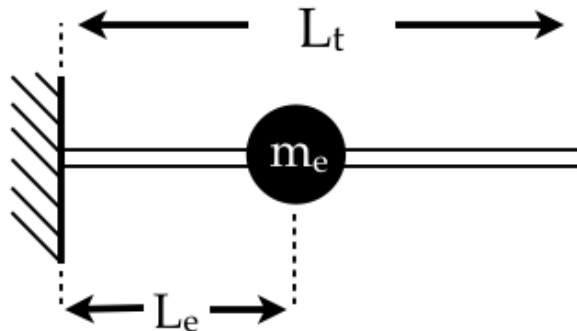


Figure A.1: Simple model of tonebar with attached actuator.

a massless beam of length  $L_e$ , shown in Figure A.2. These objects have the same fundamental vibrating frequencies as effective point masses at the end of massless beams, both of length  $L_t$ , shown in Figure A.3, where the effective mass is less than the mass of the original object and are shown for the cantilever beam and the

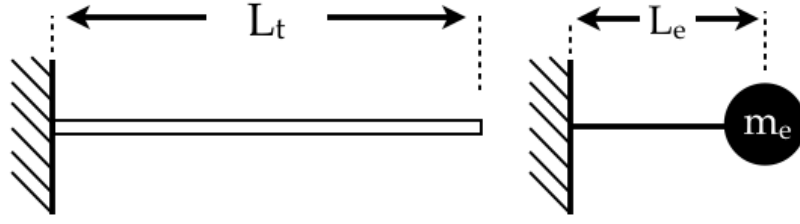


Figure A.2: Separate cantilever beam and point mass models.

electromagnet mass by Equations A.1 and A.2, respectively.

$$m_{t'} = 0.346L_twh\rho \quad (\text{A.1})$$

$$m_{e'} = m_e \left(\frac{L_e}{L_t}\right)^3 \quad (\text{A.2})$$

Finally, both of these masses can be added together (Figure A.4) and related to

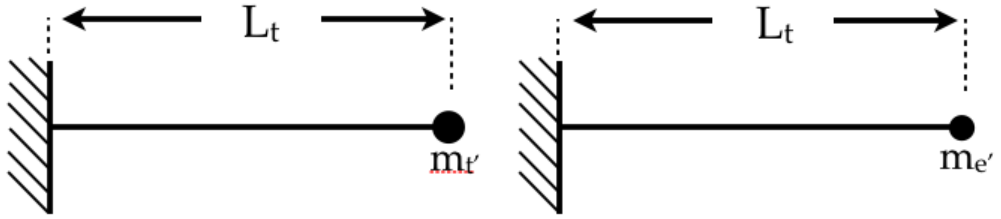


Figure A.3: Effective masses at length  $L_t$  of cantilever beam and actuator mass.

the fundamental vibrating frequency:

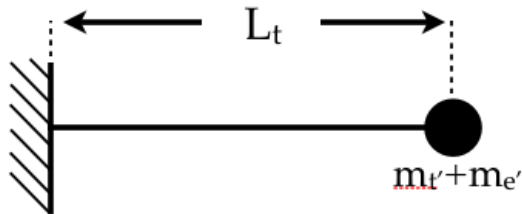


Figure A.4: Aggregate effective mass on massless beam of length  $L_t$ .

$$f_0 = \frac{1}{2\pi} \sqrt{\frac{3EK}{(m_{t'} + m_{e'})L_t^3}} \quad (\text{A.3})$$

Substituting Equations A.1 and A.2 into Equation A.3 allows us to solve for  $L_t$  in terms of the known physical dimensions and quantities of the tonebar and electromagnet:

$$L_t^4 = \frac{\frac{3EK}{(2\pi f_0)^2} - m_e L_e}{0.346wh\rho} \quad (\text{A.4})$$

# Appendix B

## Mechanical-electrical signal path

A piezo-electric sensor is attached to and accelerates with the end of the tonebar, thus experiencing a force and a resulting pressure  $P$  over the area  $A$  in contact with the tonebar and perpendicular to the direction of motion:

$$F = ma \tag{B.1}$$

$$P = \frac{F}{A} \tag{B.2}$$

This pressure deforms the piezo-electric material generating a proportional voltage which is presented at the input buffer of the electrical circuit (shown in Figure B.1).

The purpose of this circuit is to drive an alternating current through the electromagnet thus producing a magnetic field. Several of the circuit components introduce a frequency dependent delay - this delay can be measured at the excitation signal frequency and adjusted with the constant amplitude phase shifter. We will address this variable phase shift after examining the remainder of the electrical-mechanical signal path.

The magnetic field  $B$  along the axis of an electromagnet with an air core and at a distance  $z$ :

$$B(z) = \frac{\mu_0}{4\pi} \frac{NIr^2}{2(z^2 + r^2)^{\frac{3}{2}}} \quad (\text{Biot-Savart law}) \quad (\text{B.3})$$

Our electromagnet has a steel core and the magnetic field must pass through an air gap before reaching the tine. Regardless, none of these factors introduce a delay.

The magnetic force on the tine is equal to the gradient of the magnetic field  $B$  in the direction of the tine's magnetic moment  $m_B$ :

$$F_{mag} = \nabla(m_B \cdot B) \quad (\text{B.4})$$

The above equations show the only delay between the sensed acceleration of the tonebar and the exerted magnetic force on the tine is introduced by the electrical circuit and may be adjusted.

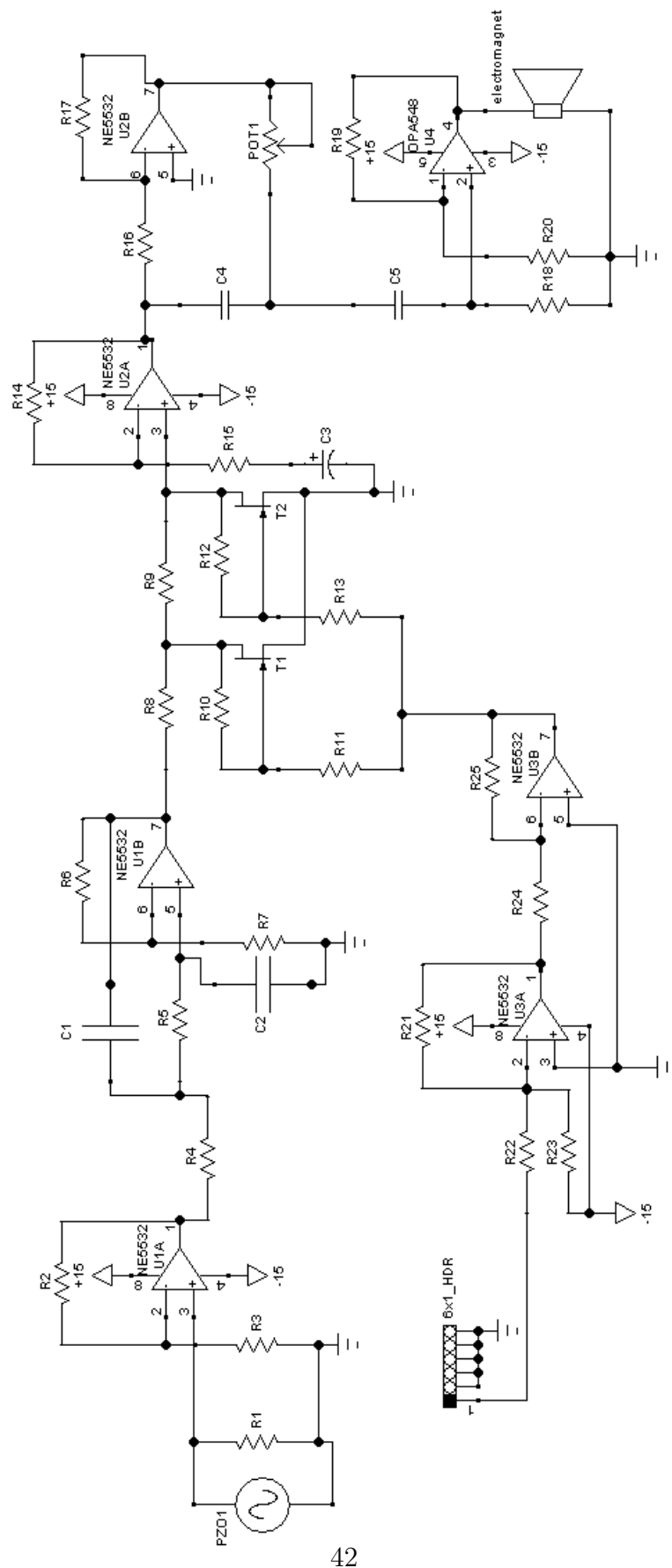


Figure B.1: Complete excitation circuit diagram for one note.